Phase I Ridge-Regularised Multivariate Coefficient of Variation Control Charts for High-Dimensional Processes Under Localised Contamination

O. A. Oyegoke[1,2], K. S. Adekeye[3], D. M. Okewole[1], O. O. Oladipupo[1], and O. I. Adegbite[1]

Phase I monitoring of the multivariate coefficient of variation (MCV) is essential for establishing stable control limits. Yet, it remains underexplored in high-dimensional settings, where classical covariance matrix estimators often become singular, and variables are correlated. This study addresses this gap by proposing a Phase I monitoring framework that uses an alternative ridge estimator (Altridge) within a penalised likelihood framework. The estimation procedure adapts the Reyment, Voinov-Nikulin, and Albert-Zhang MCV formulations to yield stable, positive-definite covariance estimates, specifically targeting scenarios with localised contamination and high- dimensionality (p≥n); using probability to signal (PTS) as a performance metric. Significant findings from extensive Monte Carlo simulations demonstrate that the proposed Altridge charts provide stable estimation and effectively detect process disturbances, with detection probability increasing alongside shift magnitudes (δ) and contamination levels (m^1). Notably, the Albert-Zhang-based chart consistently exhibits the highest sensitivity among the three methods due to a computational structure that avoids direct matrix inversion, making it more robust against numerical instability. A real-life application to a breast cancer diagnostic dataset confirms the practical implication of this framework; it successfully identifies abnormal variability patterns within a complex, correlated biomedical dataset, establishing the methodology as a reliable tool for high-dimensional Phase I process monitoring.

Keywords: High-dimensional process, Probability to signal, Likelihood ratio, Ridge regularisation, Localised contamination

DOI: https://doi.org/10.63255/04-7798.25/05

1.0 Introduction

Statistical process control (SPC) is vital for maintaining process stability across manufacturing, engineering, and healthcare sectors. Phase I monitoring serves as the critical retrospective stage of this process, focused on establishing stability and estimating parameters from historical data to ensure that control limits are not biased by outliers. While traditional multivariate SPC focuses on absolute dispersion or mean vectors, among the most established are generalised variance charts and Hotelling's T^2 (Hotelling 1947). Monitoring the multivariate coefficient of variation (MCV) is more informative in many industrial and biomedical applications where the process mean and variance are dependent.

In modern data environments, practitioners frequently encounter high-dimensional settings where the process dimension *p* is comparable to or larger than the sample size *n*. This structure introduces several critical limitations to existing Phase I literature. Classical MCV formulations such as those

[1] Redeemer's University, Department of Mathematics and Statistics, Nigeria
[2] Corresponding Email: odunayo4mine@gmail.com. The views expressed in this paper are solely those of the author(s) and do not necessarily reflect the views, policies, or official position of the Chartered Institute of Statisticians of Nigeria (CISON), its Council, Management, or any of its affiliated bodies.
[3] University of Gambia, Office of the Deputy Vice-Chancellor, Kanifing, The Gambia

by Reyment (1960) and Voinov and Nikulin (1996), rely on the inversion of the sample covariance matrix. In high-dimensional settings, this matrix becomes singular and non-invertible, rendering these traditional charts mathematically unstable. Although the Albert and Zhang (2010) method reduces dependence on direct inversion, it does not explicitly account for the estimation challenges posed by localised contamination in high-dimensional noise. Existing regularised frameworks, such as the LASSO-penalized approach used by Oyegoke *et al.* (2026), favour variable selection (sparsity). This can inadvertently ignore critical dependence structures between variables that are essential for a comparative MCV assessment.

To address these gaps, this study proposes a novel Phase I monitoring framework based on an alternative ridge-regularised (L_2-norm) approach. This methodology introduces several key contributions. Unlike LASSO-based frameworks, this approach utilises a ridge-type penalty to improve numerical stability (Oyegoke *et al.,* 2024; Teng, 2021), and it preserves important dependence structures among variables while ensuring the precision matrix remains stable and positive-definite

Three existing MCV formulations are incorporated into the regularised framework and evaluated using the probability to signal criterion. Extensive Monte Carlo simulation experiments are conducted under varying process dimensions, subgroup sizes, and shift magnitudes. The practical usefulness of the proposed methodology is further illustrated by applying it to a breast cancer diagnosis dataset.

The rest of this paper is structured as follows: Section 2 presents the multivariate coefficient of variation formulations and the proposed regularised estimation procedure. Section 3 describes the simulation design and performance evaluation framework. Simulation findings are discussed in Section 4, while Section 5 illustrates a real-life application of the proposed methodology. Concluding remarks are provided in the final section.

2.0 Multivariate Coefficient of Variation Monitoring in Phase One

The multivariate coefficient of variation for the phase I control chart is a time-based plot of the estimated coefficient of variation from a predetermined number of previous samples.
Let $Y_1, Y_2, \dots, Y_m$ be multivariate normal random variables that are independent, identically distributed, and have a covariance matrix ($\boldsymbol{\Sigma}$) and mean vector ($\boldsymbol{\mu}$), i.e., Y$\sim N_p$ ($\boldsymbol{\mu_0}$, $\boldsymbol{\Sigma_0}$), where

$$\mathbf{y}_n = \left(\mathbf{y_{n1}},\ \mathbf{y}_{n2}, \dots,\ \mathbf{y}_{np}\right)^T,\ 1 \le n \le m, \text{ and } \boldsymbol{\mu} = \left(\boldsymbol{\mu_1}, \boldsymbol{\mu_2}, \dots, \boldsymbol{\mu_p}\right)^T.$$

Reyment (1960) proposed an expression for MCV which is given by

$$\gamma_R = \left(\det(\boldsymbol{\Sigma_0})^{1/p} \ / \ \boldsymbol{\mu_0}^{\mathbf{T}}\boldsymbol{\mu_0}\right)^{-\frac{1}{2}} \tag{1}$$

and

Voinov and Nikulin (1996) expression for MCV is given by

$$\gamma_{VN} = (\boldsymbol{\mu_0}^{\mathbf{T}}(\boldsymbol{\Sigma_0})^{-\mathbf{1}}\boldsymbol{\mu_0})^{-\frac{1}{2}} \quad (2)$$

The expression in Equation (2) was established to be a generalisation of the Mahalanobis distance, which is invariant to change in scale and requires $\boldsymbol{\Sigma_0}$ to be full rank and positive definite. Since the method depends on the inverse of the $\boldsymbol{\Sigma_0}$, it becomes unsuitable for high-dimensional data.

Albert and Zang (2010) proposed an extension of the MCV presented in Equation (3), which is suitable for high-dimensional applications. Nevertheless, the measure may become unstable when elements of the mean vector are close to zero, and its performance depends on reliable covariance estimation. In high-dimensional settings, covariance estimation can become unstable or ill-conditioned, thereby affecting monitoring performance. These limitations motivate the use of regularised covariance estimators, such as the alternative ridge estimator, which provides more stable and positive-definite covariance estimates.

$$\gamma_{az} = (\boldsymbol{\mu_0}^{\boldsymbol{T}}\boldsymbol{\Sigma_0}\,\boldsymbol{\mu_0}\ /\ (\boldsymbol{\mu_0}^{\boldsymbol{T}}\,\boldsymbol{\mu_0})^{\mathbf{2}})^{\frac{1}{2}} \quad (3)$$

In a situation where μ_0 and Σ_0 are unknown, to estimate the MCV parameters in Equations (1), (2), and (3), $\boldsymbol{\mu_0}$ and $\boldsymbol{\Sigma_0}$ are replaced by their estimated values from the m historical reference sample in Phase I. The unbiased estimates for $\boldsymbol{\mu_0}$ and $\boldsymbol{\Sigma_0}$ are presented in Equations (4) and (5), respectively.

$$\bar{\mathbf{y}} = \left(\frac{1}{n}\sum_{h=1}^{n}\mathbf{y}_{h1}, \frac{1}{n}\sum_{h=1}^{n}\mathbf{y}_{h2}, \ldots, \frac{1}{n}\sum_{h=1}^{n}\mathbf{y}_{hp}\right)^{T} \quad (4)$$

and

$$\mathbf{S} = \frac{1}{n-1}\sum_{h=1}^{n}\left((\mathbf{y}_h - \bar{\mathbf{y}})(\mathbf{y}_h - \bar{\mathbf{y}})\right)^{\mathrm{T}} \quad (5)$$

The sample MCV statistic based on the estimates obtained from Equations (4) and (5), is given as follows:

$$\hat{Y}_R = \left((\mathbf{det}\,\mathbf{S})^{1/P} / \bar{\mathbf{y}}^{\mathbf{T}}\bar{\mathbf{y}}\right)^{-\frac{1}{2}} \quad (6)$$

$$\hat{Y}_{VN} = (\bar{\mathbf{y}}^{\mathbf{T}}\,\mathbf{S}^{-\mathbf{1}}\ \bar{\mathbf{y}})^{-\frac{1}{2}} \quad (7)$$

$$\hat{Y}_{AZ} = (\bar{\mathbf{y}}^{\mathbf{T}}\mathbf{S}\,\bar{\mathbf{y}} / (\bar{\mathbf{y}}^{\mathbf{T}}\,\bar{\mathbf{y}})^{\mathbf{2}})^{\frac{1}{2}} \quad (8)$$

2.1 Covariance Matrix Estimation Based on Regularised Normal Likelihood

When $n < p$, the sample covariance matrix becomes singular and non-invertible, posing challenges for high-dimensional multivariate analysis. To overcome this limitation, Oyegoke *et al.* (2024) proposed an alternative ridge ($L_2 - norm$) a regularised covariance estimator that yields a stable and positive-definite estimate of Σ given by:

$$2^{-n}ln|\boldsymbol{\psi}| - \frac{1}{2}\sum(\mathbf{y_i} - \vec{\mathbf{y}})\ \boldsymbol{\psi}(\mathbf{y_i} - \vec{\mathbf{y}})^{\mathbf{T}} \quad (9)$$

When the sample's mean vector is zero, the estimated $\boldsymbol{\Sigma}$ is:

$\widehat{\boldsymbol{\Sigma}} = \frac{1}{n}\sum \mathbf{y}_i^{\mathbf{T}} \mathbf{y}_i$; and MLE for $\boldsymbol{\psi} = \boldsymbol{\Sigma}^{-1}$ is given as:

$$\widehat{\boldsymbol{\psi}}_{MLE} = \underset{\psi}{argmin}\{tr(\boldsymbol{\psi}\mathbf{S}) - log|\boldsymbol{\psi}|\} \tag{10}$$

where the trace operator is denoted by tr (.) and the matrix's determinant by $|\cdot|$, respectively, and

$$\mathbf{S} = \frac{1}{n}\sum_{i=1}^{n}(y_{i,} - \mu_{0,})(y_{i,} - \mu_{\mathbf{0},})^{T} \tag{11}$$

when $n < p$. The following objective function can be solved to get $\widehat{\Psi}$ within the framework of penalized likelihood:

Derivation of the Precision matrix

$$\boldsymbol{\psi}_{L_2} = \underset{\psi}{argmin}\left\{\mathbf{tr}(\boldsymbol{\psi}\mathbf{S}) - log|\boldsymbol{\psi}| + \frac{\lambda}{2}\|\boldsymbol{\psi} - \boldsymbol{\psi_0}\|_2\right\}, \tag{12}$$

Equation (12) above represents the mathematical bridge between the classical estimation and the regularised framework required for high dimensionality.

2.2 The Alternative Ridge-Based Multivariate Coefficient of Variation Control Chart Under the Localised Disturbance

However, in this work, the focus is on an alternative ridge-regularised (L_2-norm) covariance estimator, while in Oyegoke *et al.* (2026), the procedure was based on a LASSO-penalized likelihood ratio framework using an L_1-norm penalty for inducing sparsity and variable selection. The motivation for this transition is the special needs of monitoring a high-dimensional process ($n< p$) for which it is more important to preserve the integrity of the correlation structure than it is to eliminate variables.

The alternative ridge-based multivariate coefficient of variation (Altridge MCV) control chart is developed to monitor relative process variability in high-dimensional processes under localised disturbances. To overcome covariance instability, when the number of quality characteristics is large relative to the sample size, an alternative ridge-regularised covariance estimator is incorporated into the charting statistic framework. The proposed chart statistics are obtained by substituting $\mathbf{S^{-1}}$ by $\boldsymbol{\psi}^{\mathbf{altridge}}$ in the MCV estimators defined in Equations 6-8.

Derivation of Altridge-based MCV:

The monitoring statistics for the three formulations by integrating the Altridge estimator:

Thus, the Altridge-based MCV Statistic based on the Reymen (1966) method is given by:

$$\hat{Y}_R = \left(\left(det\boldsymbol{\psi}_{\mathbf{L2}}^{-\mathbf{1}}\right)^{1/P} / \bar{\mathbf{y}}^{\mathbf{T}}\bar{\mathbf{y}}\right)^{-\frac{1}{2}} \tag{13}$$

Similarly, the Altridge-based MCV Statistic based on the Voinov and Nikulin (1996)

method is given by:

$$\hat{Y}_{VN} = (\bar{\mathbf{y}}^{\mathbf{T}} \boldsymbol{\psi}_{\mathbf{L2}} \bar{\mathbf{y}})^{-\frac{1}{2}} \quad (14)$$

Finally, the Altridge-based MCV Statistic based on the Albert and Zang (2010)

method is given by:

$$\hat{Y}_{AZ} = \left(\bar{\mathbf{y}}^{\mathbf{T}} \boldsymbol{\psi}_{\mathbf{L2}}^{-\mathbf{1}} \bar{\mathbf{y}} / (\bar{\mathbf{y}}^{\mathbf{T}} \bar{\mathbf{y}})^{\mathbf{2}}\right)^{\frac{1}{2}} \quad (15)$$

For ease of notation, the MCV control chart formulations based on the alternative ridge estimator (Altridge) will hereafter be referred to as the Altridge charts for MCV_R, MCV_{VN}, and, MCV_{AZ}, respectively.

The one-sided upper control limit for the MCV control chart is given as:

$$\mathrm{V}_j = \frac{\hat{\gamma}_{j.}}{\gamma}; \quad (16)$$

where *j represents R, VN, and AZ for* MCV_R *Altridge chart,* MCV_{VN} *Altridge chart,* and, MCV_{AZ} *Alridge chart*, respectively. and $\hat{\gamma}_{j.}$ are the MCV estimates based on the Altridge.

Getting V's expected value on both sides of Eq (16), we have:

Control limit Mathematics:

$$E(\mathrm{V}_j) = \frac{E(\hat{\gamma}_{j.})}{\gamma} = d_{2,(j,m,n)} \quad (17)$$

where d_2 depends on the number of variables (p), sub-group samples number (m), and the sample size (n).

This ensures that the Phase I chart is mathematically beached in its ability to fix the false alarm probability (α) across varying dimensions and sample sizes

$E(\hat{\gamma}_{Altridge})$ can be substituted with mean of samples $\hat{\gamma}_j$ $'s$ $\left(\bar{\hat{\gamma}}_j = \frac{\sum_{i=1}^{m} \hat{\gamma}_{j,i}}{m}\right)$ computed from phase I samples. Therefore, an unbiased MCV estimator can be written as:

$$\hat{\gamma} = \frac{\bar{\hat{\gamma}}_j}{d_{2,j,n}} \quad (18)$$

The upper probability bounds for the one-sided upward MCV charts for phase I are specified as follows using the notion mentioned above:

$$\widehat{UCL}_{j,m,n} = V_{m,n,} \frac{\bar{\hat{\gamma}}_j}{d_{2,j,n}} \quad (19)$$

where, $V_{m,n,j}$ is the control constant that fixes the false alarm probability (α) at a specified threshold.

3.0 Assessment of the Proposed Control Charts' Performance

Effectiveness of alternative ridge multivariate coefficient of variation (MCV) control charts was assessed using the Probability to Signal (PTS) criterion. The PTS represents the likelihood that a control chart correctly identifies the presence of a disturbance in the monitored process. The PTS metric was utilised in this investigation to compare detection performances of three regularised charting structures developed from the Reyment, Voinov-Nikulin, and Albert-Zhang formulations.

To obtain the control chart constants corresponding to a specified false alarm probability (FAP), extensive Monte Carlo simulation experiments were conducted under in-control process conditions. The simulations considered several combinations of subgroup size, process dimension, and number of Phase I samples. For each experimental setting, multivariate normal observations were generated to calculate in-control parameters and determine corresponding control limits.

Let A_i denote the event that the chart statistic corresponding to the i^{th} sample exceeds the established upper control limit. The probability that a signal is produced by a particular sample is therefore represented by:

$$P(A_i) \tag{20}$$

The overall false alarm probability for the Phase I procedure is expressed as:

$$\alpha = P(\bigcup_{i=1}^{m} A_i) \tag{21}$$

where m is the total number of samples from Phase I. PTS values were subsequently estimated under both in-control and contaminated process conditions.

3.1 Design of Monte Carlo Simulations

Experiments using Monte Carlo simulation were implemented in the R statistical programming environment to evaluate the performance of the proposed charts under varying process conditions. For each simulation configuration, 100,000 replicated Phase I datasets were generated from a multivariate normal distribution.

The simulation procedure involved the following stages:

1. For specified values of subgroup size n, process dimension p, and number of Phase I samples m, in-control multivariate observations were generated.
2. $\bar{Y}$ and S were estimated from each generated dataset.

3. The three MCV statistics corresponding to the Reyment, Voinov–Nikulin, and Albert–Zhang formulations were computed using the alternative ridge-regularised covariance estimator.
4. Control chart constants were determined for selected combinations of $m = 30$ and $m = 75$, with subgroup sizes $n = 5, 10$, and 15.
5. The upper control limits were then established to achieve the desired false alarm probability level.

The simulation framework was repeated over different parameter settings to investigate the sensitivity of the proposed monitoring schemes to changes in process dimension, subgroup size, and disturbance magnitude.

3.2 Localised Disturbance Model for the Multivariate Coefficient of Variation

To evaluate chart performance under contaminated conditions, a localised disturbance structure was introduced into the Phase I observations. Under this framework, only a subset of the Phase I samples was generated from an out-of-control process, while the remaining samples were retained under in-control conditions.

Suppose that m^1 observations originate from the in-control distribution, while m^0 samples are generated from a contaminated process. The disturbance magnitude was controlled through the shift parameter:

$$\delta \in \{1.2, 1.4, 1.6, 1.8, 2.0, 2.5, 3.0, 4.0, 5.0\}$$

where δ represents the degree of departure from the in-control multivariate coefficient of variation structure.

Therefore, the model for localised disturbance is given as:

$$m^1 = m - m^0$$

where,

m^0 = samples drawn from m in-control processes $N_P(\mu_0, \Sigma_0(\gamma_0))$

m^1 =The remaining samples which are drawn from an out-of-control process $N_p(\mu_0, \Sigma_0(\gamma_0))$

For each specified shift level, 100,000 contaminated Phase I datasets were generated and analysed using the proposed monitoring procedures. The corresponding MCV statistics were evaluated and compared against the established upper control limits. The resulting probabilities of signalling were then computed for each charting scheme.

The performance assessment focused on examining the effects of:

a. process dimension (p),
b. subgroup size (n),
c. number of contaminated samples (m_1), and
d. disturbance magnitude (δ)

on the capability of the proposed charts to detect localised shifts in process variability.

4.0 Simulation Results

Table 1: The values of V_n and $d_{2(n)}$ for various *n* and *m* values at $\alpha = 0.1. and\ p = 10$

n		$m = 30$			$m = 75$		
		VN	AZ	R	VN	AZ	R
5	V_n	0.2486	1.5486	0.2874	0.2823	1.6746	0.2954
	$d_2(n)$	0.1284	0.6542	0.2148	0.1283	0.6538	0.2149
10	V_n	0.4038	1.3101	0.5070	0.4768	1.4017	0.5362
	$d_2(n)$	0.1644	0.6478	0.2853	0.1645	0.6476	0.2853
15	Vn	0.7566	1.2326	0.7513	0.8377	1.3015	0.7806
	$d_n(n)$	0.2232	0.6712	0.3645	0.2228	0.6708	0.3642

The above table provides the control constant V_n and unbiasedness constants ($d_2(n)$) constants for the Altridge MCV charts under $p = 10$ and a fixed false alarm probability of $\alpha = 0.1$, these constants were determined for three MCV formulations across subgroup sizes of 5,10, and 15. The results showed that the V_n generally increases with *n*

Table 2: The values of V_n and $d_{2(n)}$ for various *n* and *m* values at $\alpha = 0.1, and\ p = 20$

n		$m = 30$			$m = 75$		
		VN	AZ	R	VN	AZ	R
5	V_n	0.0768	1.5910	0.1115	0.0817	1.7089	0.1133
	$d_2(n)$	0.0554	0.7322	0.0976	0.0554	0.7317	0.0977
10	V_n	0.1022	1.3472	0.1947	0.1110	1.4226	0.2017
	$d_2(n)$	0.0655	0.7074	0.1453	0.0655	0.7071	0.1453
15	Vn	0.1210	1.2034	0.2531	0.1333	1.2755	0.2731
	$d_n(n)$	0.0733	0.6678	0.1689	0.0733	0.6684	0.1688

The above table presents the $V_n$and $d_2(n)$ constants for the high-dimensional case of $p = 20$ at α =0.1. Similar to the $p = 10$ settings, these constants are used to establish the control limits of

the Altridge MCV charts. Generally, the smaller $V_n$values for the VN methods reflect the effect of increased dimensionality on the monitoring statistics.

Using the values of the control charts constants for the R, VN, AZ presented in Tables 1 and 2, the probability to signal ratio for the localised MCV disturbances is calculated for various degrees of shifts (δ) and the results are presented in Tables 3, 4, 5, and 6. It should be noted that the degree of shifts considered in this study are = {1.2, 1.4, 1.6, 1.8, 2.0, 2.5, 3.0, 4.0, 5.0}

Table 3: The PTS values of the model of localised MCV disturbances for m =30, p =10, α = 0.1 on Altridge at varying level of n and m_1.

n	δ	VN				R				AZ			
		m^1				m^1				m^1			
		3	6	9	12	3	6	9	12	3	6	9	12
5	1.2	0.1508	0.1618	0.1660	0.1593	0.1309	0.1499	0.1465	0.1508	0.3710	0.4927	0.5130	0.4942
	1.4	0.2189	0.2663	0.2860	0.2824	0.1835	0.2046	0.2244	0.2329	0.7829	0.8969	0.9147	0.9064
	1.6	0.3081	0.3886	0.3979	0.3792	0.2722	0.3060	0.3122	0.2817	0.9167	0.9854	0.9918	0.9885
	1.8	0.4046	0.5150	0.5364	0.5050	0.4183	0.4567	0.4376	0.4088	0.9479	0.9958	0.9990	0.9989
	2	0.5244	0.6156	0.6277	0.6152	0.5695	0.6273	0.5721	0.5165	0.9554	0.9978	0.9998	0.9998
	2.5	0.6626	0.7989	0.8031	0.7711	0.8495	0.8876	0.8299	0.7391	0.9577	0.9987	1.0000	1.0000
	3	0.7673	0.8758	0.8843	0.8507	0.9301	0.9700	0.9445	0.8738	0.9576	0.9987	1.0000	1.0000
	4	0.8491	0.9398	0.9440	0.9231	0.9551	0.9942	0.9914	0.9656	0.9576	0.9988	1.0000	1.0000
	5	0.8828	0.9632	0.9684	0.9540	0.9570	0.9969	0.9975	0.9877	0.9576	0.9988	1.0000	1.0000
													0.1643
10	1.2	0.1835	0.2149	0.2197	0.2062	0.1448	0.1177	0.1405	0.1474	0.1508	0.1677	0.1744	
	1.4	0.3010	0.3600	0.3613	0.3792	0.1508	0.1576	0.1694	0.1835	0.2352	0.2773	0.3116	0.2960
	1.6	0.4381	0.5326	0.5628	0.5336	0.1702	0.2038	0.2321	0.2275	0.3805	0.4540	0.4573	0.4248
	1.8	0.5690	0.6862	0.6981	0.6688	0.2414	0.2722	0.2475	0.2573	0.5894	0.6530	0.6180	0.5560
	2	0.6647	0.7892	0.8027	0.7742	0.2939	0.3422	0.3233	0.2968	0.7558	0.8178	0.7707	0.7119
	2.5	0.8077	0.9159	0.9286	0.9100	0.5125	0.5244	0.4801	0.4236	0.9283	0.9725	0.9579	0.8994
	3	0.8701	0.9612	0.9707	0.9580	0.6936	0.7184	0.6461	0.5321	0.9523	0.9945	0.9934	0.9716
	4	0.9207	0.9847	0.9910	0.9865	0.8894	0.9047	0.8281	0.7146	0.9574	0.9982	0.9994	0.9969
	5	0.9376	0.9912	0.9957	0.9931	0.9355	0.9647	0.9176	0.8058	0.9576	0.9985	0.9998	0.9993
15	1.2	0.2070	0.2204	0.2368	0.2406	0.1160	0.1043	0.1204	0.1142	0.1752	0.2014	0.2520	0.2475
	1.4	0.3396	0.4376	0.4806	0.4763	0.1097	0.1422	0.1482	0.1576	0.2573	0.3528	0.4058	0.4254
	1.6	0.5278	0.6695	0.6853	0.6633	0.1677	0.1949	0.2118	0.2204	0.3541	0.4742	0.5292	0.5761
	1.8	0.6746	0.8141	0.8191	0.8121	0.1810	0.2189	0.2383	0.2588	0.4266	0.5699	0.6203	0.6573
	2	0.7641	0.8916	0.9165	0.8909	0.2038	0.2618	0.2788	0.2982	0.5035	0.6555	0.7125	0.7254
	2.5	0.8715	0.9657	0.9779	0.9707	0.2707	0.3613	0.3886	0.3792	0.7347	0.8141	0.8315	0.8315
	3	0.9128	0.9835	0.9923	0.9902	0.3402	0.4573	0.4606	0.4584	0.8568	0.9179	0.9024	0.8835
	4	0.9391	0.9931	0.9980	0.9977	0.5292	0.5804	0.5637	0.5326	0.9474	0.9838	0.9734	0.9473
	5	0.9477	0.9959	0.9990	0.9991	0.6643	0.6674	0.6262	0.5940	0.9552	0.9938	0.9911	0.9749

The above table shows the PTS results for a process with m=30, phase I samples, and p=10. The PTS increases monotonically when the shift magnitude increases from 1.2 to 5.0 in all tested settings. Compared to the VN and R charts, the AZ Altridge chart is more sensitive to small changes; for instance, at n=5 and δ=1.4, the AZ chart reaches a PTS close to 0.90, while the others stay below 0.30, when p=n= 10, indicating that the Albert-Zhang Altridge chart offers superior

sensitivity in detecting localised disturbances, with detection performance significantly increasing as δ and m^1 increase. Moreover, all monitoring techniques generally have better detection capabilities when the number of contaminated samples increases from 3 to 12.

Table 4: The PTS values of the model of localised MCV disturbances for m =30, p =20, $\alpha = 0.1$ on the Altridge Estimator at varying levels of n and m^1.

n	δ	VN				R				AZ			
		m^1				m^1				m^1			
		3	6	9	12	3	6	9	12	3	6	9	12
5	1.2	0.1652	0.1652	0.1876	0.1826	0.2141	0.2429	0.2573	0.2498	0.8757	0.9668	0.9792	0.9767
	1.4	0.2376	0.2982	0.3088	0.2882	0.5919	0.6898	0.6709	0.6002	0.9563	0.9983	0.9999	1.0000
	1.6	0.3355	0.4347	0.4444	0.4195	0.8962	0.9577	0.9444	0.8933	0.9580	0.9987	1.0000	1.0000
	1.8	0.4551	0.5614	0.5774	0.5655	0.9508	0.9939	0.9951	0.9856	0.9577	0.9988	1.0000	1.0000
	2	0.5482	0.6766	0.6996	0.6530	0.9580	0.9977	0.9994	0.9982	0.9576	0.9988	1.0000	1.0000
	2.5	0.7155	0.8288	0.8515	0.8072	0.9586	0.9987	0.9999	1.0000	0.9576	0.9988	1.0000	1.0000
	3	0.7989	0.9047	0.9183	0.8854	0.9583	0.9988	1.0000	1.0000	0.9576	0.9988	1.0000	1.0000
	4	0.8722	0.9560	0.9633	0.9463	0.9579	0.9988	1.0000	1.0000	0.9576	0.9988	1.0000	1.0000
	5	0.8916	0.9725	0.9774	0.9642	0.9577	0.9988	1.0000	1.0000	0.9576	0.9988	1.0000	1.0000
10	1.2	0.1396	0.1677	0.1876	0.1933	0.1601	0.1876	0.1802	0.1916	0.3010	0.3880	0.3792	0.3817
	1.4	0.2853	0.3509	0.3722	0.3568	0.3335	0.4094	0.4312	0.3594	0.7603	0.8657	0.8624	0.8178
	1.6	0.4623	0.5623	0.5769	0.5730	0.6266	0.7092	0.6946	0.6238	0.9275	0.9867	0.9899	0.9794
	1.8	0.5739	0.7274	0.7311	0.6959	0.8394	0.9109	0.8773	0.8031	0.9541	0.9971	0.9992	0.9985
	2	0.7061	0.8304	0.8382	0.8170	0.9283	0.9744	0.9645	0.9185	0.9574	0.9984	0.9999	0.9999
	2.5	0.8370	0.9405	0.9484	0.9311	0.9578	0.9974	0.9987	0.9937	0.9576	0.9987	1.0000	1.0000
	3	0.8981	0.9734	0.9811	0.9688	0.9584	0.9986	0.9998	0.9994	0.9576	0.9988	1.0000	1.0000
	4	0.9321	0.9899	0.9950	0.9920	0.9581	0.9988	1.0000	1.0000	0.9576	0.9988	1.0000	1.0000
	5	0.9424	0.9941	0.9976	0.9964	0.9579	0.9988	1.0000	1.0000	0.9576	0.9988	1.0000	1.0000
15	1.2	0.1965	0.2360	0.2329	0.2337	0.1702	0.1876	0.1908	0.1965	0.1818	0.1892	0.2078	0.2149
	1.4	0.3482	0.4318	0.4312	0.4410	0.2780	0.3462	0.3436	0.3515	0.4142	0.4763	0.4758	0.4172
	1.6	0.5180	0.6443	0.6643	0.6246	0.5080	0.5752	0.5726	0.5090	0.7527	0.8183	0.7851	0.6859
	1.8	0.6699	0.8042	0.8197	0.7817	0.7283	0.8054	0.7785	0.6996	0.9124	0.9665	0.9515	0.8887
	2	0.7697	0.8871	0.9034	0.8759	0.8735	0.9296	0.9076	0.8357	0.9505	0.9932	0.9922	0.9731
	2.5	0.8872	0.9700	0.9765	0.9677	0.9538	0.9939	0.9919	0.9717	0.9587	0.9985	0.9998	0.9993
	3	0.9235	0.9867	0.9925	0.9892	0.9582	0.9981	0.9992	0.9956	0.9585	0.9987	1.0000	1.0000
	4	0.9454	0.9949	0.9984	0.9976	0.9584	0.9987	0.9999	0.9998	0.9580	0.9988	1.0000	1.0000
	5	0.9514	0.9967	0.9993	0.9991	0.9578	0.9987	1.0000	1.0000	0.9578	0.9988	1.0000	1.0000

The performance of the charts when p=20 with 30 Phase I samples is shown in the above table. The results show that the AZ Altridge chart is very robust, maintaining a PTS above 0.87 even at

the smallest shift of $\delta = 1.2$ when the subgroup size is n=5. This dominance is especially noticeable when n < p. The R and VN charts also improve with larger shifts, but they need significantly higher magnitudes to match the AZ method's detection speed.

Table 5: The PTS values of the model of localised MCV disturbances for m =75, p =10, 0.1 on the Altridge Estimator at varying levels of n and m^1.

n	δ	VN				R				AZ			
		m^1				m^1				m^1			
		7	15	22	30	7	15	22	30	7	15	22	30
5	1.2	0.1657	0.1953	0.2137	0.2293	0.1411	0.1523	0.1497	0.1765	0.5365	0.6708	0.7008	0.6755
	1.4	0.2802	0.3562	0.3477	0.3709	0.1848	0.2215	0.2026	0.2200	0.9423	0.9882	0.9903	0.9853
	1.6	0.4585	0.5494	0.5651	0.5421	0.3015	0.3509	0.3331	0.3437	0.9949	0.9999	1.0000	0.9999
	1.8	0.5789	0.7145	0.7050	0.6959	0.4277	0.4919	0.4645	0.4385	0.9987	1.0000	1.0000	1.0000
	2	0.7068	0.8314	0.8256	0.7879	0.6129	0.6644	0.6175	0.5611	0.9992	1.0000	1.0000	1.0000
	2.5	0.8735	0.9532	0.9516	0.9258	0.9081	0.9256	0.8706	0.7584	0.9994	1.0000	1.0000	1.0000
	3	0.9415	0.9853	0.9858	0.9726	0.9859	0.9911	0.9732	0.9054	0.9994	1.0000	1.0000	1.0000
	4	0.9807	0.9975	0.9976	0.9935	0.9984	0.9998	0.9989	0.9860	0.9994	1.0000	1.0000	1.0000
	5	0.9897	0.9991	0.9992	0.9976	0.9991	1.0000	0.9999	0.9972	0.9994	1.0000	1.0000	1.0000
10	1.2	0.1961	0.2446	0.2729	0.2378	0.1590	0.1454	0.1497	0.1683	0.1929	0.2385	0.2347	0.2758
	1.4	0.3690	0.4699	0.4939	0.4805	0.1765	0.1790	0.1839	0.2065	0.3324	0.4225	0.4688	0.4368
	1.6	0.5836	0.7071	0.7284	0.6925	0.1757	0.2393	0.2192	0.2010	0.5179	0.6512	0.6658	0.6271
	1.8	0.7676	0.8622	0.8757	0.8406	0.2729	0.2980	0.2909	0.2823	0.7571	0.8252	0.8107	0.7694
	2	0.8724	0.9506	0.9432	0.9221	0.3216	0.4054	0.3658	0.3496	0.9127	0.9497	0.9262	0.8749
	2.5	0.9655	0.9940	0.9944	0.9870	0.5462	0.6025	0.5332	0.4602	0.9951	0.9990	0.9967	0.9788
	3	0.9878	0.9990	0.9992	0.9978	0.7701	0.7685	0.6928	0.5716	0.9989	1.0000	0.9999	0.9979
	4	0.9963	0.9999	0.9999	0.9998	0.9584	0.9485	0.8829	0.7514	0.9993	1.0000	1.0000	1.0000
	5	0.9978	1.0000	1.0000	1.0000	0.9914	0.9881	0.9535	0.8462	0.9994	1.0000	1.0000	1.0000
15	1.2	0.2499	0.2589	0.2700	0.2888	0.1420	0.1360	0.1480	0.1590	0.2758	0.3290	0.3884	0.3853
	1.4	0.4914	0.6372	0.6491	0.5993	0.1674	0.2192	0.2293	0.2324	0.4317	0.6136	0.6617	0.7071
	1.6	0.7437	0.8661	0.8710	0.8406	0.2270	0.2909	0.3189	0.3243	0.5772	0.7635	0.8134	0.8464
	1.8	0.8776	0.9634	0.9633	0.9470	0.2736	0.3908	0.3809	0.4160	0.6745	0.8481	0.8903	0.9041
	2	0.9458	0.9896	0.9913	0.9839	0.3358	0.4553	0.4909	0.4747	0.7711	0.9088	0.9329	0.9444
	2.5	0.9875	0.9993	0.9996	0.9991	0.4520	0.6021	0.6309	0.5886	0.9278	0.9763	0.9833	0.9788
	3	0.9954	0.9999	1.0000	0.9999	0.5686	0.6833	0.7191	0.6807	0.9850	0.9952	0.9949	0.9928
	4	0.9982	1.0000	1.0000	1.0000	0.7418	0.8256	0.8220	0.7989	0.9986	0.9998	0.9996	0.9985
	5	0.9988	1.0000	1.0000	1.0000	0.8516	0.8826	0.8769	0.8388	0.9992	1.0000	1.0000	0.9996

When the total number of Phase I samples is increased to m=75, Table 5 presents the PTS results for p=10. The results shown here are in accordance with the m=30 scenarios, indicating that detection performance scales with both contamination amount and shift magnitude. The AZ method often achieves a near-perfect PTS of 1.0 at lower shift magnitudes, retaining its leadership. The table also demonstrates that, for moderate-to-large shifts, increasing the subgroup size n from 5 to 15 generally improves the sensitivity of the VN and R charts, reducing the difference with the AZ chart.

Table 6: The PTS values of the model of localised MCV disturbances for m =75, p =20, $\alpha = 0.1$ on the Altridge Estimator at varying level of n and m^1.

n	δ	VN				R				AZ			
		m^1				m^1				m^1			
		7	15	22	30	7	15	22	30	7	15	22	30
5	1.2	0.1864	0.2215	0.2293	0.2378	0.2262	0.2787	0.2794	0.2816	0.9832	0.9986	0.9992	0.9982
	1.4	0.3202	0.4137	0.3999	0.3945	0.6627	0.7333	0.7089	0.6361	0.9992	1.0000	1.0000	1.0000
	1.6	0.4898	0.5924	0.6073	0.5840	0.9639	0.9847	0.9727	0.9277	0.9994	1.0000	1.0000	1.0000
	1.8	0.6397	0.7734	0.7628	0.7185	0.9972	0.9998	0.9995	0.9947	0.9994	1.0000	1.0000	1.0000
	2	0.7683	0.8639	0.8656	0.8310	0.9991	1.0000	1.0000	0.9998	0.9994	1.0000	1.0000	1.0000
	2.5	0.9024	0.9670	0.9712	0.9504	0.9994	1.0000	1.0000	1.0000	0.9994	1.0000	1.0000	1.0000
	3	0.9576	0.9911	0.9920	0.9811	0.9994	1.0000	1.0000	1.0000	0.9994	1.0000	1.0000	1.0000
	4	0.9858	0.9986	0.9987	0.9962	0.9994	1.0000	1.0000	1.0000	0.9994	1.0000	1.0000	1.0000
	5	0.9917	0.9995	0.9996	0.9986	0.9994	1.0000	1.0000	1.0000	0.9994	1.0000	1.0000	1.0000
10	1.2	0.2176	0.2537	0.2522	0.2633	0.1774	0.1880	0.2129	0.2097	0.3690	0.4624	0.4872	0.4683
	1.4	0.4323	0.4821	0.5439	0.4893	0.3671	0.4166	0.4294	0.4060	0.9131	0.9632	0.9628	0.9271
	1.6	0.6331	0.7623	0.7727	0.7261	0.6928	0.7534	0.7199	0.6466	0.9955	0.9998	0.9998	0.9984
	1.8	0.8209	0.9095	0.9135	0.8733	0.9152	0.9473	0.9134	0.8277	0.9990	1.0000	1.0000	1.0000
	2	0.9095	0.9689	0.9686	0.9441	0.9858	0.9946	0.9859	0.9447	0.9993	1.0000	1.0000	1.0000
	2.5	0.9785	0.9973	0.9975	0.9935	0.9991	1.0000	1.0000	0.9986	0.9994	1.0000	1.0000	1.0000
	3	0.9923	0.9997	0.9997	0.9990	0.9994	1.0000	1.0000	1.0000	0.9994	1.0000	1.0000	1.0000
	4	0.9975	1.0000	1.0000	0.9999	0.9994	1.0000	1.0000	1.0000	0.9994	1.0000	1.0000	1.0000
	5	0.9985	1.0000	1.0000	1.0000	0.9994	1.0000	1.0000	1.0000	0.9994	1.0000	1.0000	1.0000
15	1.2	0.2129	0.2648	0.2670	0.2794	0.1641	0.1798	0.2065	0.2042	0.1905	0.2223	0.2324	0.2552
	1.4	0.4351	0.5695	0.6005	0.5832	0.2931	0.3715	0.3613	0.3490	0.4329	0.5275	0.5005	0.4699
	1.6	0.7185	0.8250	0.8370	0.7960	0.5811	0.6312	0.6202	0.5412	0.8199	0.8615	0.8291	0.7250
	1.8	0.8755	0.9523	0.9500	0.9175	0.8153	0.8585	0.8162	0.6981	0.9782	0.9885	0.9725	0.9094
	2	0.9458	0.9858	0.9866	0.9718	0.9483	0.9648	0.9386	0.8606	0.9970	0.9996	0.9984	0.9837
	2.5	0.9896	0.9993	0.9995	0.9981	0.9977	0.9997	0.9986	0.9856	0.9993	1.0000	1.0000	1.0000
	3	0.9961	0.9999	1.0000	0.9998	0.9993	1.0000	1.0000	0.9991	0.9994	1.0000	1.0000	1.0000
	4	0.9985	1.0000	1.0000	1.0000	0.9994	1.0000	1.0000	1.0000	0.9994	1.0000	1.0000	1.0000
	5	0.9990	1.0000	1.0000	1.0000	0.9994	1.0000	1.0000	1.0000	0.9994	1.0000	1.0000	1.0000

The simulation results for the high-dimensional, large-sample scenario of p=20 and m=75 are shown in the above Table. With PTS values exceeding 0.98 at δ=1.2 for all levels m^1 when n=5, the AZ Altridge chart in this configuration demonstrates faster disturbance detection. Even while the regularised Reyment and VN formulations exhibit more sensitivity when compared to smaller sample numbers. Overall, this table's data validates that the alternative ridge-penalised likelihood framework is highly effective for reliable Phase I baselines in high-dimensional settings.

The PTS values of the model for localised MCV disturbances of m = 30, p =10, 8 $\alpha = 0.1$ according to the Altridge Estimator at various levels of shift (δ) and m^1 for n = 5, 10, and 15; when m = 30 and 75, p =10 and 20 at various values of m^1 (see Figures 1, 2, and 3 for some selected graphs)

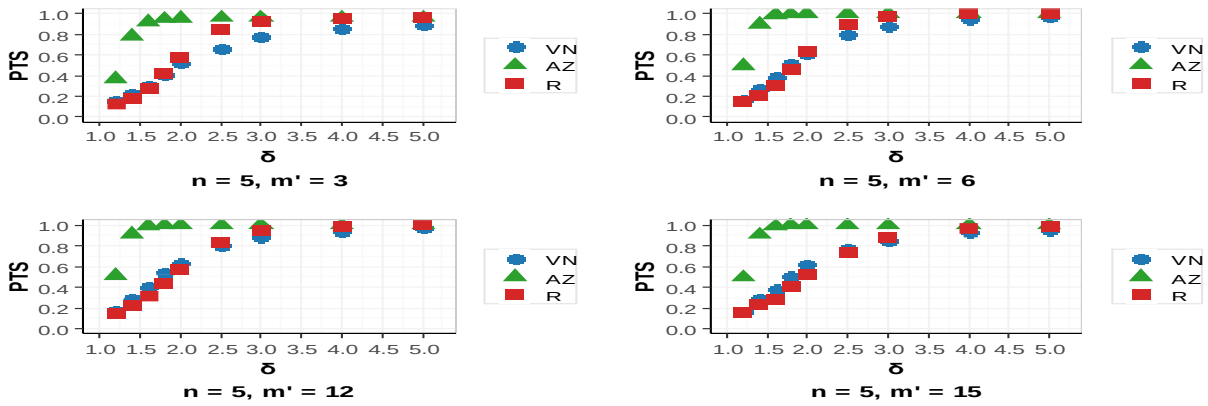

Figure 1: Illustrates detection probability (PTS) increasing with shift size (δ), and contamination (m^1), with the AZ Altridge chart showing the highest early sensitivity for p = 10, n=5, m=30 $\alpha = 0.1$

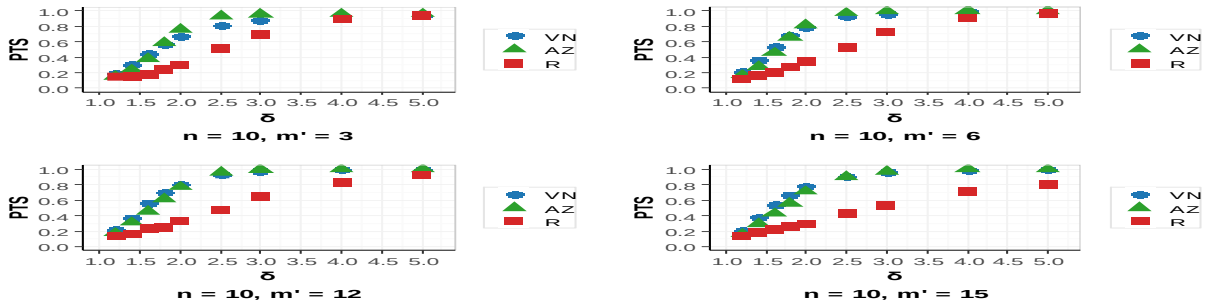

Figure 2: The PTS at various levels of m^1 at α=0.1 for p = 10, n = 10, and m = 30, and this demonstrates that increasing subgroup size (n) stabilizes monitoring statistics and enhances detection reliability.

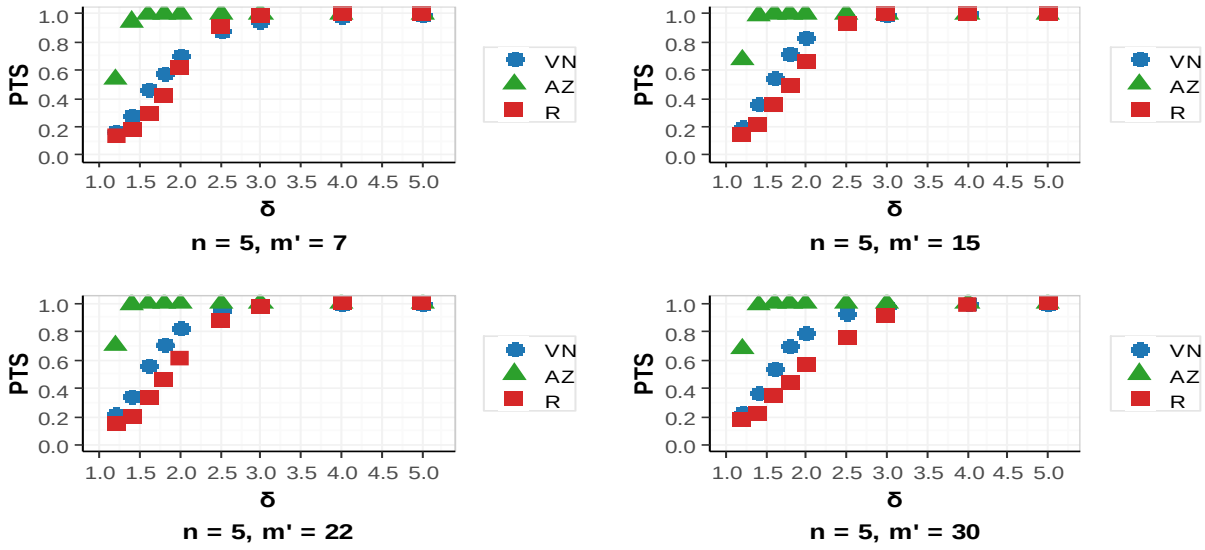

Figure 3: The PTS at various levels of m^1 at $\alpha = 0.1$ for p = 20, n =5, and m =30; highlights alternative ridge estimator's stability in high-dimensional settings where the AZ chart maintains superior sensitivity to small process shifts

5.0 Application of Proposed MCV Control Charts to real-life data

This section presents the performance of the proposed alternative ridge-regularised multivariate coefficient of variation control charts in monitoring steady-state processes and identifying localised disturbances in high-dimensional biomedical data is demonstrated by their practical application, and multivariate dataset with a focus on cell nuclei properties was used to demonstrate the proposed Phase I monitoring process. Fan *et al.* (2021) and Ebadi *et al.* (2022) used the data, which was obtained via the UW-Madison Computer Sciences Department's ftp site at http://ftp.cs.wisc.edu/math-prog/cpo-dataset/machine-learn/cancer/WDBC/. There are 569 samples total, and each measured sample has 30 real-valued quality attributes, with classification indicating whether the primary finding is malignant (M) or benign (B). There are 212 M and 357 B observations in the data set. The in-control Phase-I data consists of 357 benign (B) observations. Radius (Y1), texture (Y2), perimeter (Y3), area (Y4), smoothness (Y5), compactness (Y6), concavity (Y7), concave (Y8), symmetry (Y9), and fractal dimension (Y10) are among the measurements. As a result, the data set has ten (10) quality attributes. This suggests that p = 10 and m = 357, which were later subdivided into 35 subgroups comprising a sample size n=10. As a result, n > p, indicating that the dataset is high-dimensional and therefore suitable for illustrating the proposed charts. The estimation statistics for the three Altridge-based control charts considered in this work are displayed in Table 7. Since variables were strongly correlated, the datasets provide an appropriate framework for evaluating multivariate monitoring procedures in high-dimensional environments.

Prior to analysis, the data were screened for missing observations and standardised to eliminate scale differences among the variables. In this application, the dimensionality of the dataset is

relatively large compared with the available sample structure, thereby motivating the use of regularised covariance estimation techniques. The empirical results demonstrate that the monitored process under normal diagnostic conditions is still in control and the Albert-Zhang method has the highest sensitivity in the presence of process shifts. The three methodologies yielded estimates of the following in-control statistics: $\hat{\gamma}_{Altridge-VN} = 0.00793$, $\hat{\gamma}_{Altridge-AZ} = 0.03761$, and $\hat{\gamma}_{Altridge-R}$ =4.2058E-06.

The graphical results obtained from the proposed monitoring schemes revealed the presence of several observations exceeding the control limits, indicating potential departures from the assumed in-control structure. The findings suggest the existence of localised disturbances within subsets of the monitored observations. Among the considered methods, the results also confirm that the use of regularised covariance estimation can substantially improve the reliability of Phase I multivariate process monitoring in situations where the classical sample covariance matrix becomes unstable or ill-conditioned.

Table 7: Sample mean and Estimated MCV for Diagnostic Breast Cancer Data

Sample No.	$\overline{\mathbf{Y}}^{\mathbf{T}}\overline{\mathbf{Y}}$	$\hat{\gamma}^2_{Altridge-VN}$	$\hat{\gamma}^2_{Altridge-AZ}$	$\hat{\gamma}^2_{Altridge-R}$
1	2111897.1	0.0007854823	0.05913071	7.057901e-06
2	118465.0	0.0004269215	0.09681250	4.992633e-06
3	249771.1	0.0006575584	0.05286839	2.704788e-06
4	158716.5	0.0022070700	0.08986847	4.264425e-06
5	159083.0	0.0005910338	0.08318260	3.994916e-06
6	274746.3	0.0012793609	0.07295515	2.436430e-06
7	221553.5	0.0005464901	0.08358051	6.666894e-06
8	257845.4	0.0004931193	0.08258929	6.174393e-06
9	178515.7	0.0007976555	0.08894637	3.667941e-06
10	199253.4	0.0005735107	0.03267481	2.633735e-06
11	243742.7	0.0007694008	0.07511877	2.469524e-06
12	248305.6	0.0006218363	0.05975580	3.018852e-06
13	214668.5	0.0003621816	0.03926088	2.848575e-06
14	217202.3	0.0007753334	0.05223340	2.789897e-06
15	258464.5	0.0004127098	0.03387503	2.227459e-06
16	192994.0	0.0008476975	0.06913681	3.520317e-06
17	208893.5	0.0007393295	0.06936140	7.210951e-06
18	218846.8	0.0004967469	0.02680902	2.447922e-06

19	203506.3	0.0003488617	0.06792519	6.342970e-06
20	185599.8	0.0012932192	0.05422722	3.191526e-06
21	353111.3	0.0003813307	0.05132705	4.509362e-06
22	214855.3	0.0004745992	0.03527008	2.710567e-o6
23	222003.0	0.0008320044	0.04443416	2.624941e-06
24	236105.4	0.0005449272	0.07122283	7.743595e-06
25	176220.4	0.0005349363	0.07182191	8.7127985e-06
26	264727.3	0.0005516419	0.03703108	5.031793e-06
27	285488.4	0.0002741024	0.04042955	2.255082e-06
28	230263.7	0.0007606549	0.05348182	3.039165e-06
29	236188.2	0.0008350125	0.05848349	3.189038e-06
30	361771.2	0.0003869169	0.05527319	5.362157e-06
31	237603.1	0.0005486350	0.07691055	2.659474e-06
32	254607.4	0.0014112736	0.10327575	2.720909e-06
33	214331.7	0.0006518172	0.04880039	8.050988e-06
34	213233.2	0.0016206182	0.13668725	3.881226e-06
35	137854.1	0.0003241445	0.04652163	4.048937e-06

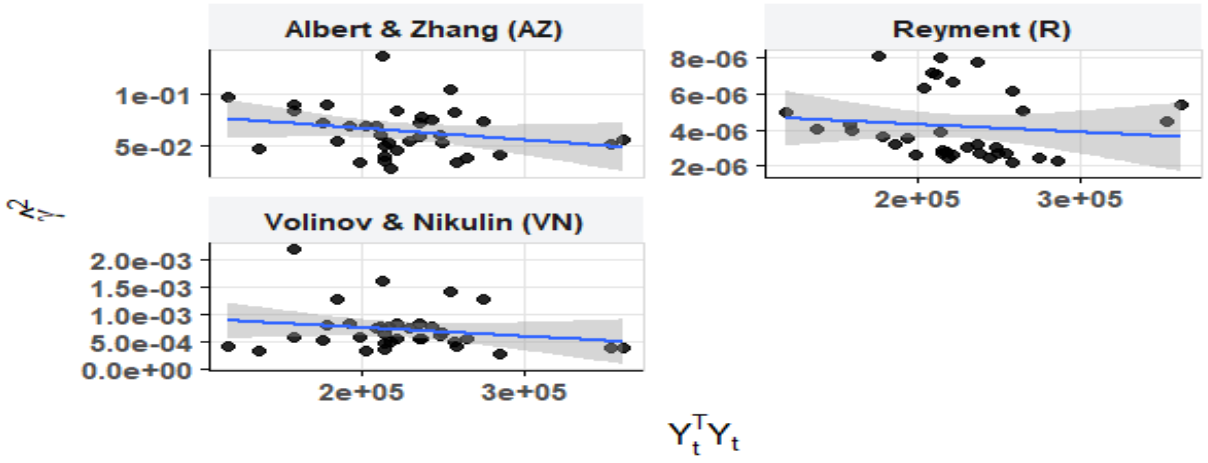

Figure 4: The above charts illustrate the scatter plot of the square multivariate CV statistic versus $\bar{y}^T\bar{y}$ regarding the breast cancer data validating the empirical assumption that MCV is constant across the observations

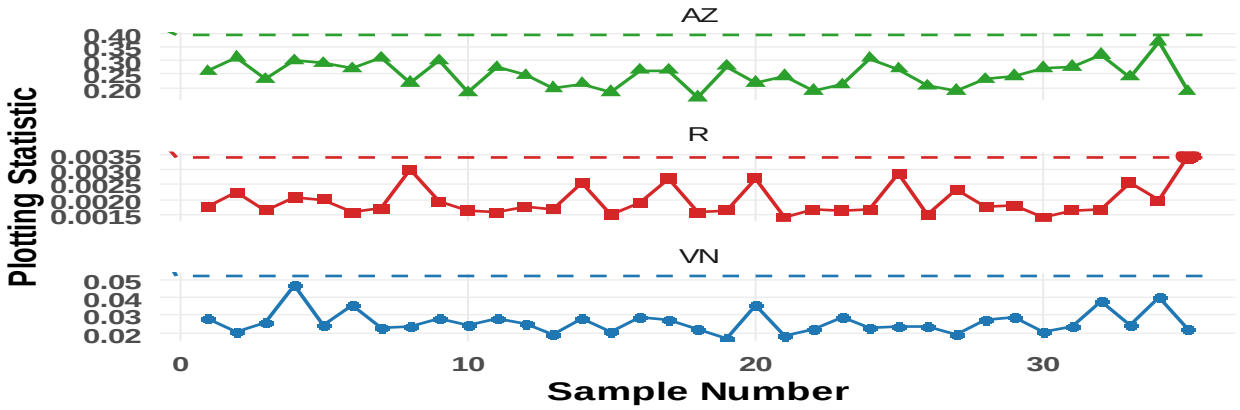

Figure 5: The three MCV charts based on Altridge for the diagnostic breast cancer data. Figure 5 shows that all plotting statistics remain below the upper control limits while utilising the Altridge-based formulations. This establishes a trustworthy baseline for Phase II monitoring by confirming that the historical process is under statistical control.

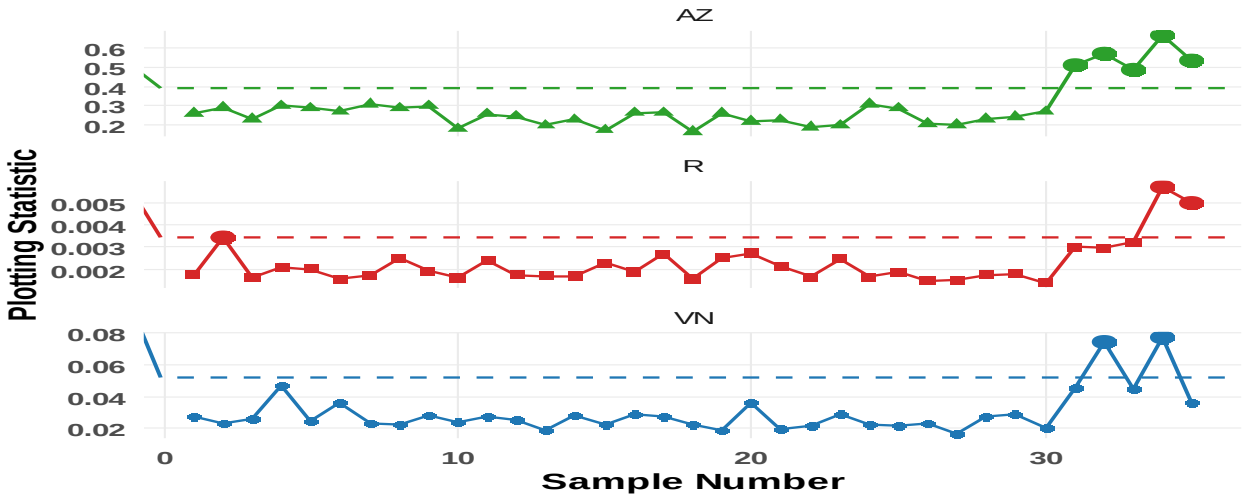

Figure 6:The chart illustrates the detection capability of the three charts when the localized disturbance at $\delta = 3$ is introduced to the last 5 samples, it provides visual evidence of AZ-Altridge chart's superior detection ability, as it provides clear outlying signals above the upper bound while other charts exhibit comparative lower sensitivity to the same shift.

6.0 Discussion of Results

The simulation results obtained in this study demonstrate that the proposed alternative ridge-based multivariate coefficient of variation control charts provide effective monitoring performance for high-dimensional Phase I processes under localised contamination scenarios. Across the different experimental configurations considered, the proposed regularised procedures consistently exhibited improved sensitivity to process disturbances while maintaining stable control chart behaviour.

The results further indicate that the monitoring performances of the proposed charts were influenced by the subgroup size, process dimension, contamination proportion, and magnitude of the induced shift. In general, larger disturbance magnitudes produced higher probabilities of signalling, indicating improved detection capability as the process moved farther away from the in-control state. The chart has been statistically significant because the PTS consistently converges to 1.0 (100% detection) as the shift magnitude δ increases. For instance, in Table 5 (p=10, n=15, $m^1 = 7$), the VN chart's PTS rises from 0.2499 at $\delta = 1.2$ to 1.0 at δ =5.0 proving a direct statistical relationship between shift size and detection reliability. Similar performance patterns were observed across the three MCV formulations considered in this study.

An important observation from the simulation analysis is that the alternative ridge-regularised covariance estimator improved the stability of the monitoring statistics in high-dimensional settings where the classical sample covariance matrix becomes unstable or singular. This improvement was particularly evident when the number of variables increased relative to the available sample size. Under such conditions. The suitability for high dimensions is specifically evidenced by Table 6, where at p=20, n=5, the AZ chart maintains a high and stable PTS, starting at 0.9832 for $\delta = 1.2$. This demonstrates that the Altridge estimator effectively prevents the charts from becoming singular or unstable, which is the limitation of classical methods.

The comparative analysis among the Reyment, Voinov-Nikulin, and Albert-Zhang formulations revealed differences in sensitivity across contamination scenarios. Although all three procedures were capable of detecting localised disturbances, the Albert-Zhang-based chart generally demonstrated relatively stronger performance in several high-dimensional configurations considered in the study, specifically as shown in Table 4 (p=20, n=5), the AZ chart achieved a PTS of 0.9563 at a small shift of $\delta = 1.4$ whereas the Voinov-Nikulin (VN) chart only reaches the PTS of 0.2376 at the same shift level. This behaviour may be attributed to its computational structure, which avoids direct inversion of the covariance matrix and is therefore less affected by numerical instability.

The empirical investigation involving the breast cancer dataset also confirmed the practical usefulness of the proposed monitoring framework. The results presented in Figure 6 demonstrate that the AZ Altridge chart could detect clear outlying signals beyond the upper control limit when a shift of $\delta=3$ was introduced into the correlated breast cancer diagnostic data, whereas the process was in-control before the shift occurred, as shown in Figure 5. The observed outlying signals suggest that the proposed procedures can successfully identify departures from the assumed in-control process structure in complex biomedical datasets characterised by strong correlations and high-dimensional variable spaces.

The findings obtained from both the simulation experiments and the real-time data applications support the suitability of the developed regularised control chart for Phase I monitoring of high-dimensional multivariate processes affected by localised disturbances. Compared with the LASSO-based approach of Oyegoke *et al.* (2026), the Altridge framework prioritises numerical stability and variable dependency retention, which makes it particularly suitable for monitoring correlated high-dimensional data.

7.0 Conclusion

This study proposed MCV control charts for a high-dimensional process in phase I using an alternative ridge-regularised covariance estimation framework. The methodology was developed to address the limitations of conventional covariance estimators in situations where the dimensionality is substantial in comparison to the sample size, particularly under localised contamination conditions.

Three multivariate coefficient of variation formulations, namely the Reyment, Voinov–Nikulin, and Albert-Zhang approaches, were incorporated into the proposed regularised monitoring framework. Their performances were evaluated using the probability to signal criterion through extensive Monte Carlo simulation experiments conducted under varying process dimensions, subgroup sizes, and contamination levels.

The results obtained from the simulation study demonstrated that the proposed ridge-based procedures were capable of effectively detecting localised disturbances in high-dimensional environments. The findings further showed that the regularisation approach improved the numerical stability of the covariance estimation process and enhanced monitoring reliability in situations where the classical sample covariance matrix becomes ill-conditioned or singular.

Utilising a real breast cancer dataset to test the proposed methods further established its practical usefulness in monitoring complex multivariate biomedical data structures. The proposed chart makes it easier to identify abnormal cellular changes early on. It is appropriate for high-dimensional diagnostic applications because it can account for correlations among features, which guarantees accurate identification of malignant tissue patterns.

The proposed regularised MCV control charts provide a useful contribution to Phase I multivariate statistical process monitoring for high-dimensional processes, especially for correlated datasets. Future research may consider extending the methodology to comparative global efficiency, diffuse shifts across all samples, non-normal process distributions, robust estimation frameworks, adaptive monitoring schemes, and dynamic high-dimensional environments involving temporal dependence structures.

Availability of Data: The dataset utilised can be found on the ftp site at the location http://math-prog/cpo-dataset/machine-learn/cancer/WDBC/ftp.cs.wsc.edu

Conflict of Interest: No conflicts of interest were declared by the authors.

Acknowledgement: The editors and the referees are highly appreciated by the authors due to the positive comments and suggestions that were made to improve the presentation of the manuscripts.

Supporting Information: The statistical analyses were conducted using the 'R' programming environment. The source code used is available with the corresponding author upon request.

References

Abbas, N., Riaz, M., Does, R. J. M. M., & Abbasi, S. A. (2018). Monitoring process parameters using a new multivariate control chart. *Quality and Reliability Engineering International, 34*(3), 489–502.

Adegoke, N. A., Adejumo, A. O., & Ogunnaike, O. (2022). A likelihood ratio-based approach for multivariate covariance monitoring. *International Journal of Quality & Reliability Management, 39*(2), 215–232.

Albert, A., & Zhang, L. (2010). A novel definition of the multivariate coefficient of variation. *Biometrical Journal, 52*(5), 667–675.

Capezza, C., Azzimonti, D., & Torti, F. (2024). On detecting out-of-control processes: A review of modern SPC techniques. *Technometrics*. https://doi.org/10.1080/00401706.2024.2327346

Castagliola, P., Achouri, A., Taleb, H., Celano, G., & Psarakis, S. (2013). Monitoring the coefficient of variation using a variable sampling interval control chart. *Quality and Reliability Engineering International, 29*(8), 1135–1149. https://doi.org/10.1002/qre.1465

Castagliola, P., Celano, G., Fichera, S., & Triantafyllou, I. S. (2011). Multivariate control charts for mean and variance using variable sample sizes. *Quality and Reliability Engineering International, 27*(3), 337–349.

Chew, X. Y. (2023). Alternative design of one-sided Shewhart control charts for the multivariate coefficient of variation. *Pertanika Journal of Science and Technology, 31*(1), 615–632. https://doi.org/10.47836/pjst.31.1.35

Giner-Bosch, V., Tran, K. P., Castagliola, P., & Khoo, M. B. C. (2019). An EWMA control chart for the multivariate coefficient of variation. *Quality and Reliability Engineering International, 35*(6), 1515–1541. https://doi.org/10.1002/qre.2459

Hotelling, H. (1947). Multivariate quality control. In C. Eisenhart, M. W. Hastay, & W. A. Wallis (Eds.), *Techniques of statistical analysis* (pp. 111–184). McGraw-Hill.

Khaw, K. W., Khoo, M. B. C., Castagliola, P., & Rahim, M. A. (2018). New adaptive control charts for monitoring the multivariate coefficient of variation. *Computers & Industrial Engineering, 126*, 595–610.

Montgomery, D. C. (2019). *Introduction to statistical quality control* (8th ed.). Wiley.

Oyegoke, O. A., Adekeye, K. S., Olaomi, J. O., & Malela-Majika, J. C. (2024). Hotelling T^2 control chart based on minimum vector variance for monitoring high-dimensional correlated multivariate processes. *Quality and Reliability Engineering International, 41*(2), 765–783. https://doi.org/10.1002/qre.3687

Oyegoke, O. A., Adekeye, K. S., & Malela-Majika, J. C. (2026). Phase I multivariate coefficient of variation control chart for high-dimensional processes. *Quality and Reliability Engineering International*, 1–14. https://doi.org/10.1002/qre.70192

Reyment, R. A. (1960). *Studies on Nigerian Upper Cretaceous and Lower Tertiary Ostracoda: Part 1. Senonian and Maastrichtian Ostracoda*. *Stockholm Contributions in Geology, 7*, 1–238.

Teng, L. (2021). Modern approaches to statistical process control in manufacturing. *International Journal of Production Research, 59*(14), 4220–4235.

Voinov, V. G., & Nikulin, M. S. (1996). *Unbiased estimators and their applications* (Vol. 2, *Multivariate case*). Kluwer Academic Publishers.

Yeong, W. C., Lim, C. P., & Chan, K. Y. (2016). Identification of special causes in industrial process monitoring. *Procedia CIRP, 45*, 123–128.

APPENDIX

TABLE OF SYMBOLS

p	Number of quality characteristics
n	Number of subgroup size
m	Number of historical reference samples
$\boldsymbol{\mu}$	True process mean vector
$\boldsymbol{\mu_0}$	In-control process mean vector
$\boldsymbol{\Sigma_0}$	In-control process covariance matrix
$\boldsymbol{\Sigma}$	True covariance matrix
$\boldsymbol{y_n}$	An observation vector rep. nth sample
$\bar{\boldsymbol{y}}$	The sample mean vector
S	The sample covariance matrix
$\boldsymbol{\Psi}$	Precision matrix
$\boldsymbol{\Psi_{L2}}$	The alternative ridge regularized precision matrix derived using the $(L_2 - \text{norm})$
$\boldsymbol{\Upsilon_R}$	The MCV formulation based on the Reyment method
$\boldsymbol{\Upsilon_{VN}}$	The MCV formulation based on the Voinov-Nikulin method
$\boldsymbol{\Upsilon_{AZ}}$	The MCV formulation based on the Alber-Zhang method
$\widehat{\boldsymbol{\gamma}}_{\boldsymbol{J}}$	The sample MCV statistic for j (where j=R, VN, AZ)
$\boldsymbol{V_J}$	Upper control limit statistic for the j^{th} MCV chart
$\boldsymbol{d_2}$	Control constant
$\boldsymbol{\lambda}$	The tuning parameter
$\boldsymbol{\delta}$	The shift magnitude
$\boldsymbol{m^1}$	The number of contaminated samples
PTS	Probability to signal
$\boldsymbol{\alpha}$	The false alarm probability